Title	High-resolution radio continuum observations of compact planetary nebulae
Author(s)	Aaquist, OB; Kwok, S
Citation	The Astrophysical Journal, 1991, v. 378 n. 2, p. 599-610
Issued Date	1991
URL	http://hdl.handle.net/10722/179671
Rights	Creative Commons: Attribution 3.0 Hong Kong License

THE ASTROPHYSICAL JOURNAL, 378:599–610, 1991 September 10

HIGH-RESOLUTION RADIO CONTINUUM OBSERVATIONS OF COMPACT PLANETARY NEBULAE

O. B. AAQUIST[1] AND SUN KWOK
Department of Physics and Astronomy, University of Calgary, Calgary, Alberta, Canada T2N 1N4
Received 1991 January 2; accepted 1991 March 20

ABSTRACT

We report 15 GHz radio continuum observations of 19 compact planetary nebulae. The high resolution ($\sim 0''.1$) images obtained allowed detailed examination of the structures of these nebulae. Most of these objects have very high radio surface brightness temperatures and critical frequencies, suggesting that they are very young planetary nebulae. Most show a "bipolar" central structure, consistent with an ellipsoidal shell viewed at an angle, and may also show extended halo structure outside of the shell, probably representing remnant material left over from the asymptotic giant branch progenitor.

Subject headings: nebulae: planetary — stars: radio radiation — nebulae: structure

1. INTRODUCTION

Conventional studies of planetary nebulae have concentrated mostly on objects which are extended in angular size, and relatively little work has been done on compact planetary nebulae. This has been due in part to the fact that many planetary nebulae are too small to be resolved by optical telescopes. However, compact planetary nebulae are interesting objects to study because among them are many young planetary nebulae early in their process of evolution. They often possess properties (e.g., strong infrared excess and molecular emission) that are characteristic of their asymptotic giant branch (AGB) progenitors. Such links have allowed us to probe the origin of planetary nebulae and how they evolve from the AGB (Kwok 1982). It is therefore important to identify a population of young planetary nebulae from which systematic studies can be made. Between 1983 and 1987 we have made a systematic survey of compact planetary nebulae that are stellar in appearance in the optical. The Very Large Array (VLA)[2] in its largest configuration can achieve angular resolution better than $0''.1$, and most compact planetary nebulae will be resolved at such angular resolution. A report of the survey of ~ 200 nebulae at 5 GHz has been given in Aaquist & Kwok (1990, hereafter Paper I). In this paper we present the results of complementary observations at 15 GHz of 19 nebulae.

The 19 program sources in the present study were selected from the sources in the 5 GHz survey which were poorly resolved at 5 GHz and had sufficiently high surface brightness temperatures to offer adequate signal per beam area at 15 GHz. The primary purpose of making these observations is to determine (1) the source structure in greater detail, (2) the optically thin density level, and (3) a better estimate of the critical frequency at which the spectrum goes from optically thick to optically thin. The 19 sources presented here are among the highest surface brightness Galactic planetary nebulae known. With the exception of Hb 12, this is the first time that these objects have been studied with such high resolution.

In § 2 the observations and data processing will be briefly described. In § 3 each of the sources is examined on an individual basis, and the physical parameters for each source are discussed in light of the new high-resolution images. In § 4 the present data are combined with existing fluxes at other wavelengths to determine the critical frequencies and spectral indices of the objects.

2. OBSERVATIONS AND RESULTS

The observations reported here were made with the VLA in the A-configuration at various times over a four year period starting 1983 August and ending 1987 September. The data were taken in the "snapshot" mode with on-source time of 15 to 20 minutes. The observing procedure was similar to that used in the 5 GHz survey in Paper I. Subsequent image processing consisting of final editing of visibility data, map making, CLEANing (sidelobe removal), self-calibration, and image and visibility analysis was performed using the Astronomical Image Processing System (AIPS). Uniform weighting and no taper were adopted. The synthesized beam has a full width half-maximum (FWHM) of $\sim 0''.1$. The typical rms noise level in the maps is ~ 0.2 mJy per beam area.

The sources observed are listed in Table 1. The first two columns identify the source by its PK designation and common name, respectively. Other names used for these sources are given by Acker, Marcout, & Ochsenbein (1983). The next two columns show the frequency band (C = 5 GHz and U = 15 GHz) and observing dates. Column 5 lists the flux density of the observed planetary nebula estimated using the AIPS task IMEAN and the averaged visibility data extrapolated to zero baseline. Because most of the sources are small, both methods usually give consistent flux values to within a few percent. Since all of our sources have high surface brightness, the statistical errors in flux are small. We believe that the major sources of error are systematic in nature, for example, from absolute calibration. Based on our experience of the VLA, we conservatively estimate the errors associated with the sources to be $\sim 10\%$. For easy reference, the 5 GHz fluxes from Paper I are also listed in Table 1.

Column 6 gives an estimate of the diameters (2θ) of the 5 and 15 GHz radio images. For sources that are well resolved, the angular diameters were estimated from the 10% intensity level in the maps. For the poorly resolved sources a Gaussian deconvolution was performed, and the resultant Gaussian

[1] Postal address: Department of Mathematics and Astronomy, University of Winnipeg, Manitoba, Canada, R3T 2N2.

[2] The Very Large Array of the National Radio Astronomy Observatory (NRAO) is operated by Associated Universities, Inc., under cooperative agreement with the National Science Foundation.

TABLE 1

OBSERVED PARAMETERS

PK Mame (1)	Name (2)	Band (3)	Date[a] (4)	F_ν (mJy) (5)	2θ (6)	T_b (K) (7)	T_c (K) (8)	M_i(10 kpc) ($M_\odot$) (9)	IRE (10)
353−4.1	H1-36	U	B	72	0.″6	1600	260	1.1(−2)	8.5
		C	B	50	0.8	5500			
1−6.2	SwSt-1	U	B	175	1.1	1100	215	4.4(−2)	5.1
		C	B	130	1.3	5500			
27+4.1	M2-43	U	L	241	1.3	1100	180	6.7(−2)	3.6
		C	G	148	1.5	4700			
30+4.1	K3-6	U	L	80	0.7	1300	140	1.5(−2)	2.5
		C	D	55	0.7	8000			
19−2.1	M4-10	U	L	31	0.9	300	<130	1.4(−2)	>2.1
		C	I	33	1.2	1600	>85		<4.1
19−5.1	M1-61	U	L	110	1.6	300	145	6.2(−2)	2.6
		C	E	97	1.8	2100			
48+1.2	K3-29	U	L	65	0.9	600	155	2.0(−2)	3.5
		C	I	58	1.0	4100			
52+2.1	K3-31	U	E	35	1.0	300	155	1.7(−2)	2.1
		C	D	39	1.5	1200			
45−1.1	K3-33	U	E	15	1.0	100	215	1.1(−2)	9.1
		C	D	17	1.1	1000			
37−6.1	NGC 6790	U	J	290	1.7	800	235	1.1(−1)	2.0
		C	D	240	1.8	5300			
42−6.1	NGC 6807	U	E	27	0.8	300	155	1.1(−2)	2.0
		C	B	29	0.8	3200			
56−0.1	K3-42	U	E	15	1.5	50	135	2.1(−2)	2.7
		C	D	19	1.2	900			
54−2.1	M1-72	U	E	31	0.6	700	140	7.5(−3)	5.0
		C	D	26	0.7	3800			
67−0.1	K3-52	U	L	80	0.7	1300	125	1.5(−2)	4.3
		C	E	65	0.7	9400			
64−2.1	K3-53	U	E	66	0.7	1100	160	1.4(−2)	3.5
		C	D	50	0.8	5500			
71−2.1	M3-35	U	E	140	1.3	700	180	5.1(−2)	2.6
		C	B	130	1.5	4100			
89−5.1	IC 5117	U	E	210	1.5	700	175	7.7(−2)	3.4
		C	B	175	1.5	5500			
100−8.1	Me2-2	U	E	38	1.0	300	185	1.8(−2)	1.7
		C	B	40	1.2	2000			
111−2.1	Hb 12	U	A	170	0.5	5800	185	1.3(−2)	<6.8
		K	A	275	0.4	5700			
		C	B	45	0.7	6500			

[a] Codes for the dates are given in Table 1 Paper I.

angular diameter was multiplied by 1.8 (Panagia & Walmsley 1978) in order to estimate the equivalent 10% contour diameters.

Column 7 gives the radio brightness temperature (T_b) defined by

$$T_b = (c^2/2\pi k\nu^2)(F_\nu/\theta^2) .$$

In most cases we find that T_b is lower at 15 GHz than at 5 GHz, suggesting that the nebulae may be optically thin at 15 GHz.

Column 8 gives dust color temperature (T_c) which is the Planck temperature obtained from least-squared fits to the *IRAS* broad-band fluxes. Column 9 gives the ionized masses of the nebulae at a distance of 10 kpc. They are calculated using the formulae in Milne & Aller (1975) and assuming a filling factor of 0.6. Since the distances are unlikely to be larger than 10 kpc, these values can be considered as upper limits to the ionized masses.

In column 10 is the calculated infrared excess (IRE) defined by

$$\mathrm{IRE} = (F_{\mathrm{IR}}/10^{-14}\ \mathrm{W\ m^{-2}})[F_\nu(15\ \mathrm{GHz})/\mathrm{mJy}]^{-1} , \quad (2)$$

where F_{IR} is the total flux emitted in the dust component. This equation is derived from equation (VII-II) of Pottasch (1984) in the high-density approximation. Positions of the sources can be found in Paper I.

The contour plots of the brightness distribution for each of the program sources are shown in Figure 1. The PK number and a common name are shown in the upper right corner of each map. The FWHM synthesized beam is represented by an ellipse in the upper left corner. Decreasing contours are indicated by "hatched" lines and negative contours by dashed lines. The peak flux and the absolute values of the contours are given in the caption below each map in janskies per beam. The contour levels are chosen according to the measured rms level in some blank area of the final map. Usually the first contour was chosen at the three rms level.

From the derived properties of the nebulae given in Table 1, we can see that these nebulae are different from the general population of planetary nebulae in several ways. First of all, the radio surface brightness temperatures are very high, which is the reason why they are selected. Second, the T_c are higher than the typical values of 40–100 K for evolved planetary nebulae (Pottasch et al. 1984), suggesting that the dust component is still close to the star. Third, the IREs are much

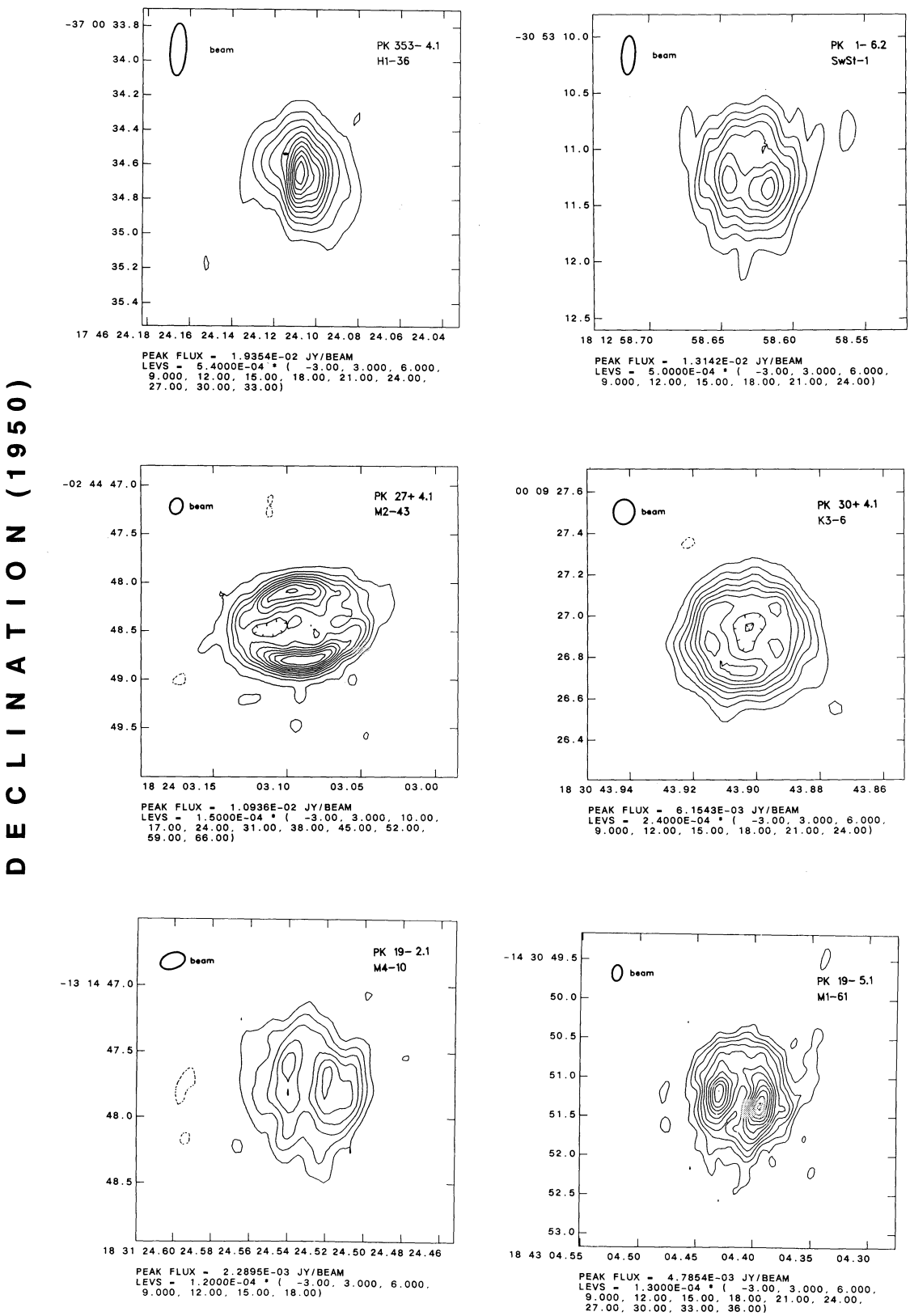

FIG. 1.—15 GHz radio continuum maps for 18 of the program sources. Peak fluxes and the estimated rms noise levels are indicated below each of the individual maps. Contour levels (also given below each map) are expressed in units of the rms level. FWHM synthesized beam is shown on the upper left corner of each map.

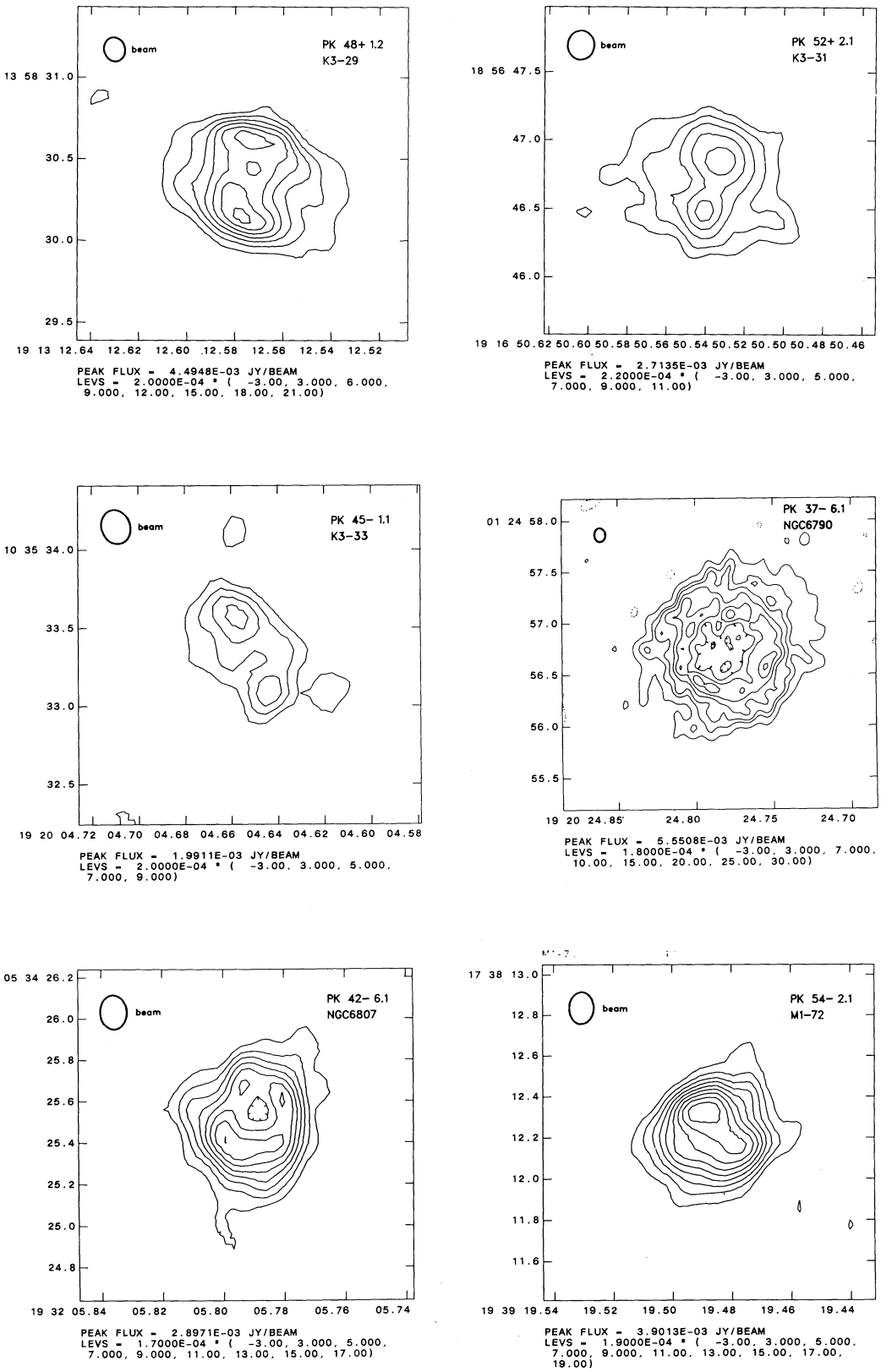

FIG. 1.—*Continued*

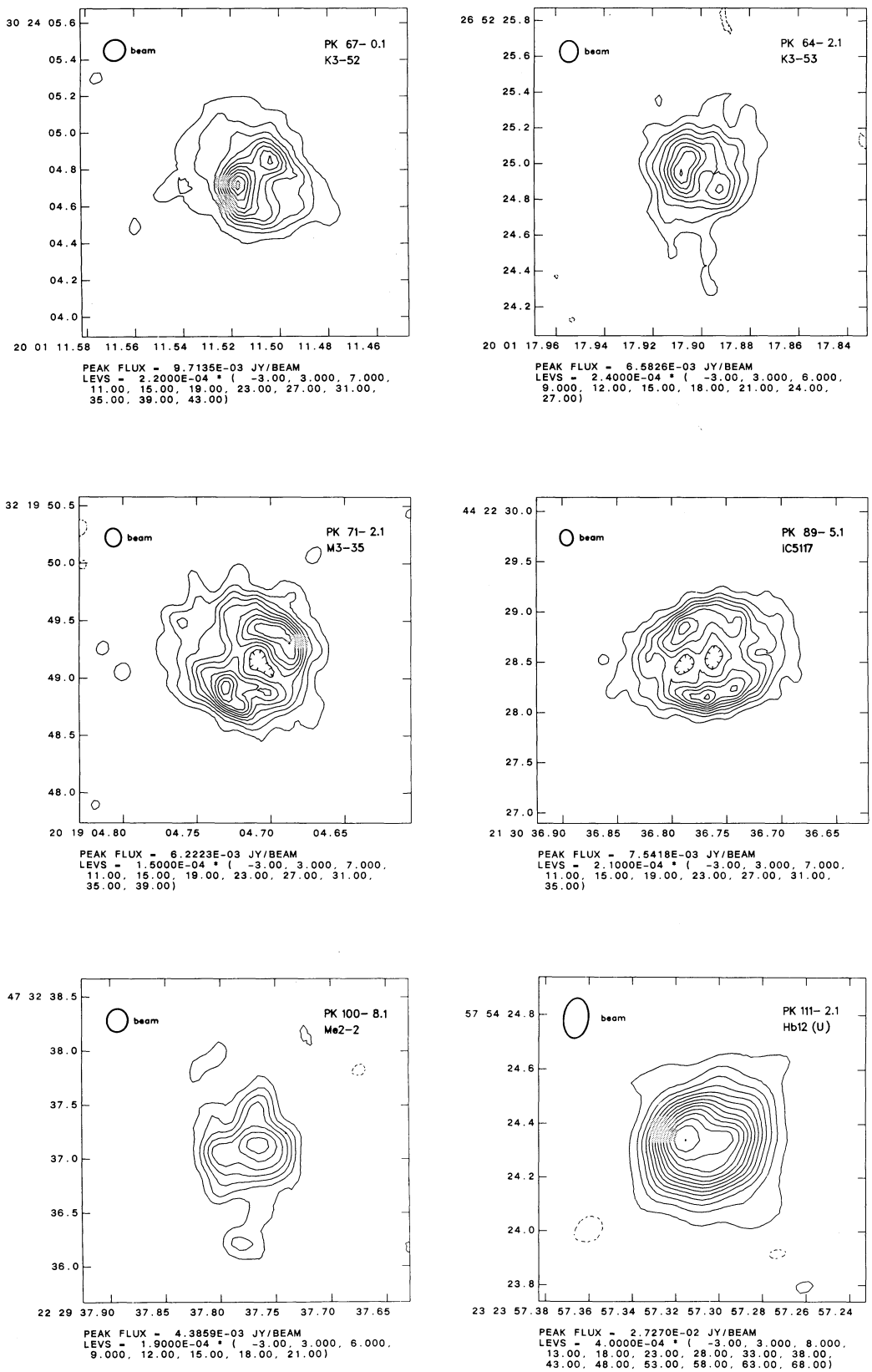

FIG. 1.—*Continued*

greater than unity, suggesting that the dust is primarily still heated by nonionizing photons and the central star temperatures are low. Last, the ionized masses are very small. Since the individual distances are not known, only upper limits can be derived (assuming $D = 10$ kpc). Since the ionized mass decreases as $D^{-2.5}$, the mass of all these nebulae are substantially lower than the traditionally assumed values of 0.2 $M_\odot$. Such small values result from either nebulae being ionization bound or the shell masses increasing with age (Kwok 1983). Both interpretations suggest that these nebulae are young systems.

3. INDIVIDUAL OBJECTS

Each of the sources in Table 1 will be discussed in some detail. Seven of the 19 sources (H1-36, SwSt-1, NGC 6790, NGC 6807, IC 5117, Me 2-2, and Hb 12) are reasonably well studied, the rest much less so.

H1-36.—While this object has been cataloged as a planetary nebula (Henize 1967; Sanduleak 1975), it is now known to be a symbiotic star (Allen 1983). Our radio fluxes are consistent with the previous measurements of Purton et al. 1982 (46 ± 10 and 90 ± 10 mJy at 5 and 15 GHz, respectively).

The radio image is poorly resolved in the north-south direction where the beam FWHM is 0".33, because of the low declination. However, in the east-west direction the FWHM is 0".1. In this direction, a brighter core surrounded by a fainter halo can be seen. There seems to be some indication of a secondary brightening 0".2 west on the peak flux position indicating a biaxial or shell-like symmetry, but the highly elliptical beam shape makes this interpretation difficult. A core-halo type structure is also inferred from the small spectral index.

A triple-source structure was reported by Taylor (1988), who interprets it to be due to a binary system with a binary separation of 0".5. Such structure is not evident in our snapshot map of H1-36.

The radio data show that this object is optically thin at about 15–20 GHz, so the IRE of 8.5 is probably not an upper limit. This high IRE is similar to other symbiotic novae such as HM Sge and V1016 Cygni. Its high (260 K) dust temperature is also more typical of symbiotic novae than planetary nebulae (Bryan & Kwok 1991).

SwSt-1.—The physical conditions in this object have recently been studied by Flower, Goharji, & Cohen (1984) and de Freitas Pacheco & Veliz (1987). SwSt-1 is a compact planetary nebulae with a low-excitation spectrum of type II in the classification scheme of Peimbert (1978). The central star is of type WC, with a Zanstra temperature of 30,000–36,000 K. The stellar continuum is well defined by *IUE* observations, and a color temperature of 42,000 K was estimated by Zhang & Kwok (1991). The presence of silicate grains (Aitken et al. 1979) and a C/O ratio of 0.72 ± 0.1 (Flower et al. 1984) implies an O-rich envelope. It has a high-density envelope ($N_e = 1.0 \pm 0.2 \times 10^5$ cm^{-3}) with an electron temperature (T_e) of $11{,}400 \pm 500$ K, and a high emission measure and critical frequency. All these properties point to a young system.

The optical lines show P-Cygni characteristics indicating the presence of a wind (de Freitas Pacheco & Veliz 1987). This wind has also been detected in the ultraviolet by Cerruti-Sola & Perinotto (1985).

Because of the low declination of this object, our radio data had poor phase stability, and the shape of the source was somewhat sensitive to the choice of self-calibration parameters. The radio data do show SwSt-1 to be resolved and have some internal structure, indicating that it is becoming optically thin at 15 GHz. The IRE and the dust temperature are quite high (Table 1), confirming that SwSt-1 is very young.

Because of its apparent early stage in evolution, together with the fact that it has an O-rich envelope as well as a high color temperature, SwSt-1 is a likely candidate for being an OH maser source. OH emission has been searched for by Payne, Phillips, & Terzian (1988) but not detected.

M2-43.—Optical spectroscopic observations show M2-43 to be a low-excitation planetary nebulae with no He II (λ4686) present and strong [O III] lines. Further, it has a steep Balmer decrement ($X > 25$) probably due to reddening (Stenholm & Acker 1987). The radial velocity is very high at 112 ± 5 km s^{-1} (Schneider et al. 1983). Its log (Hβ) flux of -13.10 ± 0.05 (Acker, Stenholm, & Tylenda 1989) coupled with an optically thin radio flux of 240 mJy gives it a rather high-extinction coefficient of 3.0.

The *IRAS* LRS show a mixed dust chemistry with both O-rich and C-rich grains present (Zhang & Kwok 1990). The object has been observed for OH maser emission but not detected (Zijlstra 1990, private communication).

The 15 GHz map in Figure 1 shows a classical planetary nebula shape, which can be explained most simply as a prolate ellipsoidal shell. Its appearance is very similar to the Ring Nebula in Lyra, which has a much lower 5 GHz brightness temperature. The emission peaks are very well defined, and it may be possible to use these peaks to observe slight changes over the period of a few years as the object evolves (Masson 1986).

K3-6.—Comparing the red and infrared colors, Sabbadin (1986) concludes that this object is a planetary nebula or an H II region. The spherical shell-like geometry shown in Figure 1 leaves little doubt that this is a planetary nebula, probably of low excitation (Greig 1972).

This is the only object in our sample that shows a perfect circular shell geometry. A slice across the center of the source fitted with a theoretical slice from a uniform density shell shows that the object is well enough resolved to rule out an end-on ellipsoid. The well-defined shell structure gives an excellent illustration of the fact that planetary nebula shells are dynamically confined from both inside outside by winds (Kwok 1982).

M4-10.—This is a confirmed planetary nebula (Sanduleak 1975). It has a radial velocity of 64 ± 5 km s^{-1} (Schneider et al. 1983). The new radio data indicate that M4-10 is optically thin at 5 GHz. The 5 GHz map is poorly resolved, and it is not clear if it has circular or ellipsoidal symmetry. The 15 GHz map, however, clearly shows a biaxial object, but the surface brightness is too low to give good structural definition. The 15 GHz map suggests that the ionized region is not constrained by a thin shell along the minor axis, implying that the nebula is density bounded. Only one good *IRAS* flux (at 25 μm) exists for M4-10, which is unusual for compact planetary nebulae. Using the fluxes at the other bands as upper limits we obtain $2.1 < \text{IRE} < 4.1$ and $84 < T_c < 130$ K.

M1-61.—The central star temperature is quite hot at 121,000 K (Iijima 1981), and the intensities of [He II] λ4686 and [O III] λ5007 relative to Hβ (Kaler 1976) place this object in a medium- to high-excitation class. The electron density is 6400 cm^{-3}, and the electron temperature is 9800 K (Tylenda et al. 1989). Tylenda et al. measured the stellar continuum at two wavelengths for this (and other objects) and found the stellar

spectrum to be much steeper than a hot blackbody of infinite temperature. This may be due to the inaccuracies of the subtraction of the nebular component if it is bright compared to the stellar component. In view of the radio images presented here, this is likely to be the case since their entrance pupil was $4'' \times 4''$ which is large compared with the diameter of the radio emission.

The extinction coefficient, based on the Balmer decrement, in 1.09 (Tylenda et al. 1989). This is consistent with that calculated using the Hβ flux from Acker et al. (1989) and the 15 GHz radio flux from Table 1.

The 15 GHz image shows a shell structure with two pronounced emission peaks which are optically thin, or nearly so. These two peaks are also apparent in the 5 GHz map. The 5 GHz map suggest an outer halo component, which major axis seems to be along a different direction than the inner shell. This effect can also be seen in K3-29 and He2-447.

K3-29.—From the $R-I$ color, Sabbadin (1986) concludes that this object is a planetary nebula or H II region. The very regular ellipsoidal shell-like geometry shown in Figure 1 leaves little doubt that this is a planetary nebula.

At 5 GHz the object is barely resolved, and no structure can be seen except for the existence of a low-level emission at position angle $+45°$ (Paper I). At 15 GHz K3-29 takes on the apperance of a very regular prolate ellipsoidal shell with a major axis nearly perpendicular to the line of sight. A closer examination of the 5 and 15 GHz images indicates that the major axis of the outer halo is slightly different from the major axis of the inner structure seen in the 15 GHz map.

K3-31.—From the $R-I$ color, Sabbadin (1986) concludes that this object is a planetary nebula or H II region. The 5 and 15 GHz maps show biaxial symmetry with the northern most intensity peak being slightly brighter than the other. The emission profiles along the axes indicate a structure similar to, but weaker than, K3-29, discussed above. Its *IRAS* color temperature, position in the *IRAS* color-color diagram, and radio morphology are all consistent with K3-31 being a planetary nebula.

K3-33.—Sabbadin (1986) concludes that this object is a planetary nebula or H II region based on the $R-I$ color. K3-33 appears distinctly retangular at 5 GHz, which is indicative of a high minor axis density relative to that along the major axis. The object may be associated with 1612 MHz OH maser emission (Eder, Lewis, & Terzian 1988). This emission is weak and of type II with a peak-to-peak separation of 25.4 km s^{-1} and a V_{lsr} of 53.4 km s^{-1}. In the *IRAS* [60 − 25]–[25 − 12] color-color diagram, K3-33 lies above the blackbody line and within the OH/IR star strip. Its color temperature and IRE are quite large, indicating that this is a very young and dusty object.

Purton & Blackwell (1991) measured 26 ± 3 and 19 ± 7 mJy at 5 and 10.6 GHz, respectively, using a single dish. In comparison, fluxes of 15 and 17 mJy at 5 and 15 GHz are measured in our survey. The excess flux at 5 GHz is probably due to confusion because of the proximity of the source to the Galactic plane. Alternatively, it may be due to some very extended radio emission. However, this would mean that there is as much flux coming from the halo as there is from the main body of the nebula, implying that the halo would have to be very extensive (greater than 12″ in diameter) in order to have gone unnoticed by the VLA. The *IRAS* position is 28″ away from the radio position, so there is some chance that the infrared flux and the maser emission are not associated with this radio source.

Based on the available data, K3-33 is of great interest and should be examined in greater detail. As a first step, the line-of-sight association of the radio position with OH emission should be confirmed; however, this will be difficult because the OH emission is weak. It would also be useful to obtain optical data on K3-33 in order to compare the optical expansion velocity with that seen in the OH maser.

NGC 6790.—The object is a medium excitation (excitation class 5) planetary nebula (Aller & Czyzak 1983) and a class C nebula (Greig 1971). The high-excitation line [He II] λ4686 seen in the spectrum is thought to originate in the central star rather than in the nebula. Mendez, Kudritzki, & Simon (1984) derive a blue magnitude of 14.46 but note that the spectrum of NGC 6790 is masked by strong nebular emission lines. Cerruti-Sola & Perinotto (1985) searched for fast stellar winds in a number of planetary nebulae, but for this object they could not see any measurable stellar continuum against which to detect a P Cygni wind. From the optical recombination and forbidden lines, the following parameters are derived: $c = 1.25$ (Balmer decrement), $N_e = (0.4\text{–}1.1) \times 10^4$ cm^{-3}, and $T_e = (1.13\text{–}1.40) \times 10^4$ K (Tylenda et al. 1989; Feibelman & Aller 1987; Kaler 1986). Phillips (1984) finds an extinction of $E_{B-V} = 0.62$ ($c = 0.91$) toward the nebula with no indication of large internal extinction. However, Köppen (1977) finds that the internal extinction is quite high. French (1983) notes that there is "a consistent—and substantial—lack of agreement among different investigations of this object. Since it is bright and nearly stellar, neither poor data nor stratification effects seem a plausible explanation. It is possible that this object is evolving on a short time scale, and monitoring over the next few years might be very valuable." A similar concern is also expressed by Aller & Czyzak (1983). The central star temperature falls in the range $43{,}000 < T_* < 80{,}000$ K (Gurzadyan 1988). The N/O ratio of 0.35 and the He/H abundance ratio suggest that the progenitor star is of intermediate mass (Sabbadin 1986; French 1983).

Gathier, Pottasch, & Goss (1986) and Taylor, Gussie, & Pottasch (1990) find H I absorption against the radio continuum associated with the planetary nebula which could be interpreted to imply the presence of an extended neutral halo. However, H_2 emission was not detected by Beckwith, Persson, & Gatley (1978), nor was CO detected by Huggins & Healy (1989). Payne et al. (1988) found no OH maser emission, which is less surprising since this object is carbon rich (Zuckerman & Aller 1986).

The diameter of the optical image of NGC 6790 has been quoted as high as 8″ (Phillips 1984), yet the radio image is only one-fourth this size, indicating that the nebula may be density bounded, unless the optical halo is due to reflection rather than recombination. If the halo is caused by fluorescence, then the total radio flux contribution cannot be more than a few mJy, otherwise its presence would have been noticed in our visibility data. An examination of the spectrum from the optical halo is required in order to determine its nature.

The 5 GHz radio image (Paper I) is poorly resolved, showing only a slight central depression and an elongation in the NW-SE direction, along the major axis of the 15 GHz image. The major axis diameter in the 5 GHz image is slightly longer (by about 1″) than that seen in the 15 GHz image. However, the minor axis width is the same at both frequencies, indicating that the nebula is ionization bounded in the direction of the minor axis. It is possible, however that it is density bounded along the major axis, which is directed at about 30° from the

line of sight. The relatively high spectral index suggests that there is very little radio emission beyond the radio image.

NGC 6807.—This is a medium-to-low-excitation object (excitation class 5) with an electron temperature of 1.12×10^4 K, electron density of 4×10^3 cm^{-3}, extinction coefficient of 0.64 (Balmer decrement), log (Hβ) flux of -11.46, optical diameter of 2″, and central star type "Of" (Aller & Keyes 1987). Schneider et al. (1987) looked for neutral hydrogen but found none.

Although this object has been observed at several frequencies (Isaacman 1984; Milne & Webster 1979; Milne & Aller 1982), the flux values are too uncertain to determine a spectral index. The critical frequency is estimated to be ~ 5 GHz. The 5 GHz image shows no structural detail. The 15 GHz image reveals a spherical shell structure reminiscent of a prolate ellipsoidal shell viewed edge-on.

K3-42.—The 5 GHz image shows this object to be a partial shell. The 15 GHz image has too low a surface brightness to form a useful image; therefore, it was not included among the images of Figure 1. A single dish measurement of 43 ± 5 mJy at 5 GHz (Purton & Blackwell 1991) is twice as high as the VLA measurement at the same frequency. This discrepancy is probably due to confusion (see discussion for K3-33 above). The object has the lowest 5 GHz brightness temperature of the sample, as well as a low color temperature, and it is optically thin below 5 GHz. Only two good *IRAS* fluxes are available. These factors may indicate that it is a more evolved planetary nebula.

M1-72.—No continuum is detected near the strong Hα line, and the [N II] line is clearly absent. The optical diameter is estimated to be less than 10″ (Henize 1967). The log (Hβ) flux is -12.54 ± 0.07 and shows an inner bright optical core of 0.″8 (Acker et al. 1989). The electron density and temperature are 3.5×10^3 cm^{-3} and 1.43×10^4 K, respectively, and the extinction constant is 2.43 (Tylenda et al. 1989).

M1-72 is only partially resolved in the 5 GHz image. At 15 GHz, M1-72 shows a typical biaxial structure seen in many planetary nebulae. The radio diameter is consistent with the inner bright optical core. If the optical halo is ionized, then the radio flux contribution from it cannot be more than a few mJy, since otherwise it would have been seen in the radio data.

Based on the radio image, there is little doubt that M1-72 is a planetary nebula.

K3-52.—From the $R-I$ color, Sabbadin (1986) concludes that this object is a planetary nebula or H II region. At 15 GHz, the object is clearly resolved, revealing a biaxial symmetry with one minor axis peak being significantly stronger than the other. A radio halo, extending beyond the minor axis peaks, is clearly visible. Other nebuale with typical prolate ellipsoidal shell morphology which tend to show an extended, clearly detectable, radio halo beyond the minor axis are M1-4 (Fig. 1, Paper I), He2-440 (Fig. 1, Paper I), and M4-10 (Fig. 1). Since K3-52 lies above the blackbody line in the *IRAS* color-color diagram, just below the area occupied by H II regions, it could be a compact H II region or an evolved planetary nebula. However, the high 5 GHz brightness temperature and high IRE seem to rule out the latter option.

K3-53.—From the $R-I$ color, Sabbadin (1986) concludes that this object is a planetary nebula or H II region. The radio data are of somewhat poor quality due to unstable phase data. The source shown in Figure 1 was recovered by self-calibration the data using the clean components from a small box surrounding the expected source position (based on the 5 GHz survey data). The image may therefore be unreliable. It is very similar in appearance to K3-52, in the degree of weakening in one of the two brightness peaks and the distribution of the extended emission. However, given that the source is located below the blackbody line in the *IRAS* color-color diagram, and that it has a high T_b, T_c, and IRE, it is most likely a planetary nebula.

Engels et al. (1985) found no evidence for OH maser emission at 1612 and 1667 MHz down to a 3 σ level of 0.3 and 0.6 Jy, respectively.

M3-35.—This object has a very sharp Hα emission line of medium intensity with no continuum near the line (Henize 1967). Later studies of line emission from this object determine that it is of moderate excitation ($T^* = 60{,}000$ K, Kaler 1986; $T_* < 102{,}000$ K, Iijima 1981). M3-35 has been searched for atomic hydrogen (Schneider et al. 1987) and OH maser emission (Lewis, Eder, & Terzian 1987; Payne et al. 1988) without success.

The ratio data available for this source indicate that it turns optically thin between 5 and 10 GHz. At 15 GHz, this structure is clearly resolved. The deep central emission minimum and the "concave" contours surrounding the peaks imply that this is a prolate ellipsoidal shell structure with the major axis rotated toward us by about 60°. There is a significant brightness enhancement at the SW end of the nebula, indicating greater densities in that direction. The 5 GHz image shows an object of about the same size with a low-level emission extending in the NE direction, implying a larger spectral index than the one calculated in Section 4. Most likely, the 2.4 GHz flux (Turner & Terzian 1984) used to determine α is too high, perhaps because of confusion.

IC 5117.—This appears to be a very dense nebula with $N_H = 20{,}000$ cm^{-3}. The [N II] and [O III] line ratios suggest even higher densities. The electron temperature ranges between 11,800 and 14,500 K, $c = 1.3$, and the excitation is higher (Aller & Czyzak 1983). Acker et al. (1982) report that the central star is of type WR (which is indicative of low excitation). Greig (1971) reports it as a class C object (indicating medium to low excitation). Kaler (1976) finds $c = 1.38$ (Balmer decrement) and [He II]/H$\beta = 0.13$, implying an excitation class of 7 (intermediate excitation). Sabbadin (1986) calculates a Zanstra temperature of $75{,}000 < T_* < 90{,}000$ K.

The optical diameter of 3″ (Acker et al. 1982) is twice the radio diameter, indicating the presence of low extended emission or a neutral reflective shell. IC 5117 was included in the pointed *IRAS* observations to search for infrared extended emission around planetary nebulae; however, none was found (Leene & Pottasch 1988). Zhang & Kwok (1991) estimate that 50% of the total flux from this object comes from the dust component, which is among the highest of all planetary nebulae. Since the dust emission is expected to decrease as the nebula expands, this suggests that IC 5117 is a very young planetary nebula.

Circumstellar CO emission was detected in IC 5117 by Huggins & Healy (1989). The measured expansion velocity of CO is 16 km s^{-1}, which is smaller than the expansion velocity (19 km s^{-1}) of H I as measured by Taylor et al. (1990).

Kohoutek & Martin (1981) report that large differences in the continuum flux and in the Hβ flux (a factor of 2) exist, as measured by other authors and themselves. They propose that an increase in the brightness of the nebula occurred between the years 1977 and 1980. However, we note that existing radio data do not show a similar increase over the same period of

time. Previous radio measurements of IC 5117 are 190 ± 40, 250 ± 40, and 140 ± 40 mJy at 10.7, 6.7, and 3.2 GHz, respectively (Higgs 1971); 198 ± 15 mJy at 5 GHz (Johnson, Balick, & Thompson 1979); 198 ± 15 and 238 ± 5 mJy at 5 and 10.6 GHz, respectively (Kwok, Purton & Keenan 1981); and 32.4 and 305.9 mJy at 1.5 and 5 GHz, respectively (Isaacman 1984). These values, and those measured by us, are generally consistent except for those of Isaacman.

The 15 GHz map shows an optically thin shell structure similar to the optical image of the Ring Nebula. The spectal index of 1.8 implies that there is little or no radio emission beyond the bounds of the radio image. This is confirmed by noting that the 5 GHz image has about the same size as the higher frequency image, although it is slightly more extended toward the east.

Me2-2.—This is a low-excitation object, with an optical diameter of 4″ and electron densities of 4×10^3 cm^{-3} (Aller & Keys 1987) and 1.8×10^4 cm^{-3} (Barker 1978). The electron temperature is (1.1 and 1.32) $\times 10^4$ K for [O III] and [N II], respectively (Kaler 1986).

The 15 GHz radio map shows the typical planetary nebula morphology which is noticeably skewed and not fully resolved. The extended low-level emission in the north-south direction seen in Figure 1 is confirmed by the 5 GHz map.

Hb 12.—The object was first noted by Purton et al. (1982) for its relatively high critical frequency and low spectral index. It was recently discussed in detail by Miranda & Solf (1989) and Dinerstein et al. (1988). Hb 12 is surrounded by a weak, circular, 26″ diameter Hα halo. The [N II] emission line shows a 0.″9 central core and a faint 10″ diameter bipolar halo. The expansion velocity of the core is ~16 km s^{-1}. The 10″ bipolar lobes, which represent mass outflow, are inclined to the line of sight and have a positive radial velocity gradient. The weak Hα halo, identifiable with the circumstellar envelope produced in the AGB stage, seems to be expanding at a slightly lesser rate of 13 km s^{-1}. Simultaneous near-infrared observations in H I recombination lines and H_2 emission lines show that the angular extent of the H_2 emission is about 8″–10″ while the ionized core is less than 2″. Examination of the relative line intensities reveals that the H_2 line emission is due to fluorescence rather than to shocked material. The neutral gas density is estimated to be 10^4–10^5 cm^{-3}.

Spectroscopic observations indicate that electron temperatures range from 1.0 to 2.2×10^4 K, densities range from 10^3 to 10^4 cm^{-3}, and both low- and high-excitation components are present (Barker 1978; Aller & Czyzak 1983). The stellar temperature is 44,000 K (Kohoutek & Martin 1981). The fraction of total flux emitted in the dust component is extremely high (55%, Zhang & Kwok 1991), confirming that this object is a very young planetary nebula.

Hb 12 was also observed by us at 23 GHz with the VLA. The derived flux density and the intensity map are shown in Table 1 and Figure 2, respectively. Previous VLA radio observations of Hb 12 have been made by Johnson et al. (1979), Newell & Hjellming (1981), and Newell in 1982 (see Bignell 1983). The VLA maps at 1.4 and 5 GHz show a central, poorly resolved object with wings extending outward in the shape of the shallow "V," with an overall extent of 10″ (Newell & Hjellming 1981). These lobes can also be seen in our 5 GHz data at the 2 rms level (Fig. 3, *left frame*) although they are more prominent in the map published by Bignell (1983).

At 5 GHz, the V-shaped halo contributes about 20 mJy of flux, and the 0.″7 core contributes 45 mJy. Based only on our VLA measurements, the spectral index of the core component alone is 1.2 ± 0.1, implying that the outward flow observed in the wing structure has its origin deep in the core. At 15 GHz the core is resolved into two components oriented approximately perpendicular to the extended wings. At 22 GHz (Fig. 2, *right frame*), the west component is seen to be optically thin while the east component is still thick and may remain so to a critical frequency of 30 ± 10 GHz. If Hb 12 is a planetary nebula, then the brightness peaks represent material swept up by a fast wind from a central star located somewhere between them. The dense east component and the less dense west component must somehow interact with the fast wind to give rise to the V-shaped flow. The large circular Hα halo shows that the original AGB material has much less pronounced density gradients.

If Hb 12 represents a stage in the development of a planetary nebula, then Hb 12 must be very young. If it is very young, then supposedly it will in the near future evolve into a more classical looking planetary nebula like the other program objects. In order it to do this, the extended shallow V-shaped emission must fade, the critical frequency must drop, and the spectral index must increase. The central core already has double and skewed emission peaks seen in many compact planetary

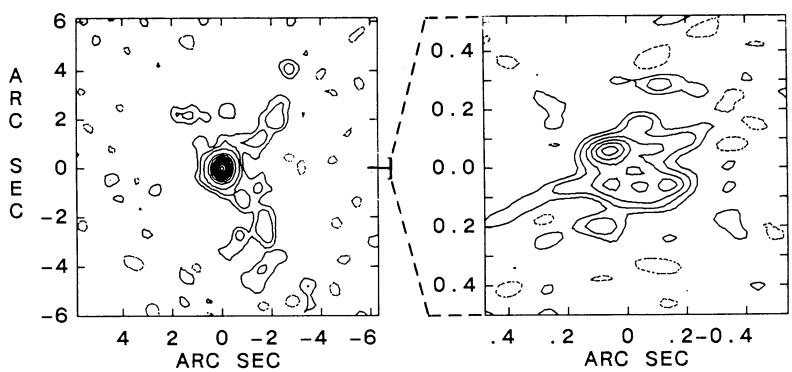

FIG. 2.—The 5 (*left*) and 22 GHz (*right*) maps of Hb 12. For the 5 GHz map, contour levels are at constant intervals of 25 times the rms noise level (0.1 mJy) from 10 to 260 times rms, plus additional contours at −2, 2, and 4 times rms. For the 22 GHz map, the contour levels are −2, 2, 4, 7, 10, 13, and 16 times the rms noise level (2.3 mJy).

nebulae; however, it is doubtful that a simple prolate ellipsoidal shell model could be constructed to fit the observed core structure.

4. RADIO SPECTRA

The possiblity of using the radio surface brightness as a distance-independent indicator of nebular age has been discussed by Kwok (1985). Another physical parameter which can serve as an age indicator is the critical frequency (ν_c) at which the spectrum becomes optically thin (Kwok et al. 1981). As a planetary nebula ages and expands, its electron density decreases, and the nebula becomes optically thin at lower frequencies. Table 2 lists other flux measurements for the nebulae in our survey sample at selected frequencies. Also included in Table 2 is the compact planetary nebula K3-35, which is described in detail in a separate paper (Aaquist 1991). For eight of the 20 nebulae, there exist enough flux measurements at other frequencies for ν_c to be determined. The radio spectra of these eight objects are plotted in Figure 3. The optically thick and optically thin parts of the spectra were fitted separately with two power laws. For the optically thin regime, the power-law index is fixed at -0.1. The derived power-law index for the optically thick part of the spectrum would correspond to the spectral index (α). The value of ν_c is determined by the cross-over of the two lines. The derived values of ν_c and α are given in each of the diagrams in Figure 3. The uncertainties in ν_c are defined as half the difference between the intersection points of the extremum lines calculated from the uncertainties of the two power-law fits. Another seven objects (K3-6, M2-43, NGC 6807, M1-72, K3-52, K3-53, and Me-2) each have one low-frequency measurement which is significantly less than that expected from the optically thin component. This suggests that the spectrum turns over within the observed spectral range. However, ν_c and α cannot be determined from a single measurement.

While this sample is too small to draw significant statistical conclusions, we nevertheless note that there is a trend of increasing values of α as ν_c decreases. Figure 4 shows a plot of ν_c versus α. The only exception to this trend is Hb 12, which has a well-defined spectral index of ~ 1 and a very high critical frequency of 28 GHz.

A correlation between ν_c and α is expected in the interacting stellar winds model of Kwok et al. (1978). During the early stages of planetary nebula evolution, most of the ionized mass is in the form of the remnant of the wind from its asymptotic giant branch progenitor. Since the wind has an inverse-squared density profile, the spectral index is expected to be ~ 0.6 (Wright & Barlow 1975). As more of the wind is swept up and compressed into a shell, the spectral index will approach the value of 2 expected of a uniform density shell. It is interesting to note that the observed range of α for this sample is indeed between 0.6 and 2. The evolution of the radio spectrum in the interacting stellar winds model is discussed in Kwok & Purton (1979).

5. CONCLUSIONS

In this paper, we have presented high-resolution radio continuum maps of 18 compact planetary nebulae. The angular resolution (0".1) is among the highest ever obtained for Galactic nebulae, allowing the detailed structure of these compact nebulae to be revealed for the first time. Fifteen of the eighteen compact planetary nebulae observed have a "bipolar" morphology showing two approximately equally prominent peaks seperated by a few tenths of an arcsecond. This is consistent

TABLE 2

MEASUREMENTS AT OTHER SELECTED RADIO FREQUENCIES

OBJECT	F_ν (mJy)								
	1.5 GHz	2.7 GHz	5.0 GHz	6.2 GHz	8.1 GHz	8.9 GHz	10.6 GHz	15 GHz	22 GHz
H1-36	...	33 ± 4[a]	46 ± 10[a]	65 ± 10[a]	82 ± 7[a]	90 ± 15[a]	...	...	...
SwSt-1	...	63 ± 3[a]	148 ± 15[b]	...	...	...	...	240 ± 27[c]	128 ± 93[a]
M2-43	...	...	118 ± 11[d]	...	...	...	236 ± 6[d]	233 ± 27[e]	...
K3-6	...	...	45 ± 12[d]	...	...	...	85 ± 8[d]	...	...
K3-31	...	...	38 ± 3[d]	...	...	...	36 ± 5[d]	...	...
K3-33	...	...	26 ± 3[d]	...	...	...	19 ± 7[d]	...	...
NGC 6790	48.7 ± 4.8[f]	160 ± 60[g]	256 ± 30[c]	...	...	...	340 ± 60[h]	...	...
K3-35	...	20 ± 0.4[k]	39 ± 2[d]	...	...	...	58 ± 5[d]	57 ± 1[k]	56 ± 3[k]
NGC 6807	11.5 ± 1.2[f]	...	22 ± 7[c]	...	...	...	150 ± 70[h]	28 ± 16[e]	...
K3-42	...	...	43 ± 5[d]	...	...	...	18 ± 5[5]	...	...
M1-72	...	...	21 ± 3[d]	...	...	...	31 ± 3[d]	...	...
K3-52	...	...	...	...	...	...	86 ± 3[d]	...	...
K3-53	...	...	53 ± 6[d]	...	...	...	73 ± 3[d]	...	...
M3-35	...	...	117 ± 7[d]	...	...	...	169 ± 3[d]	...	...
IC 5117	32.4 ± 3.2[f]	...	198 ± 15[i]	...	...	...	238 ± 50[j]	...	...
Me2-2	16.1 ± 1.6[f]	...	53 ± 11[i]	...	...	...	...	...	...
Hb 12	...	27 ± 3[a]	64 ± 6[i]	...	...	81 ± 3[a]	122 ± 20[a]	...	201 ± 27[a]

[a] Purton et al. 1982.
[b] Milne 1979.
[c] Milne & Aller 1975.
[d] Purton & Blackwell 1991.
[e] Milne & Aller 1982.
[f] Isaacman 1984.
[g] Milne & Webster 1979.
[h] Higgs 1971.
[i] Johnston et al. 1979.
[j] Kwok et al. 1981.
[k] Aaquist 1991.

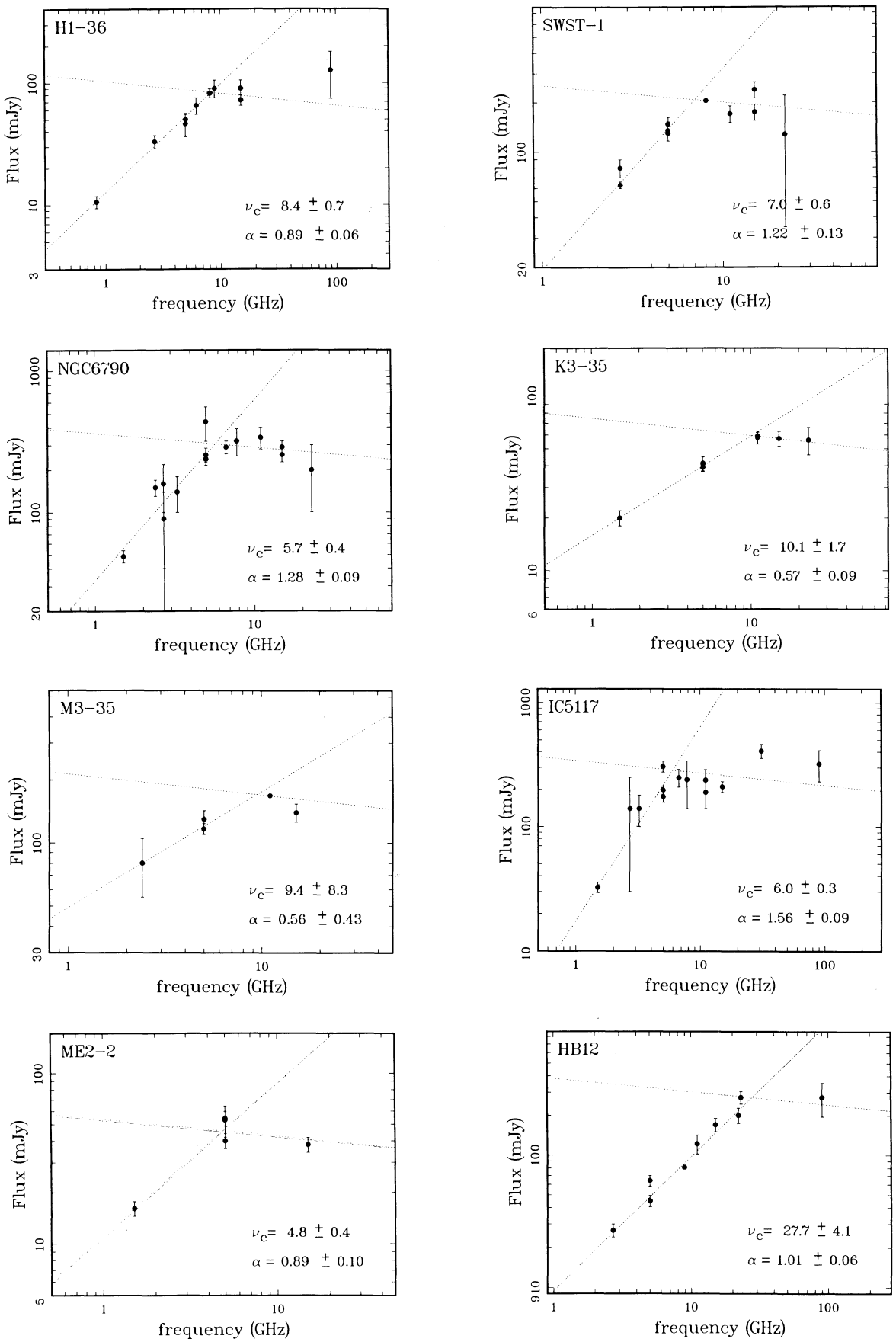

FIG. 3.—Radio continuum spectra of eight compact planetary nebulae. The two dotted lines represent least-square-fitted power laws to the optically thick and optically thin components. Derived critical frequencies and spectral indices are given in the lower right corner of each diagram.

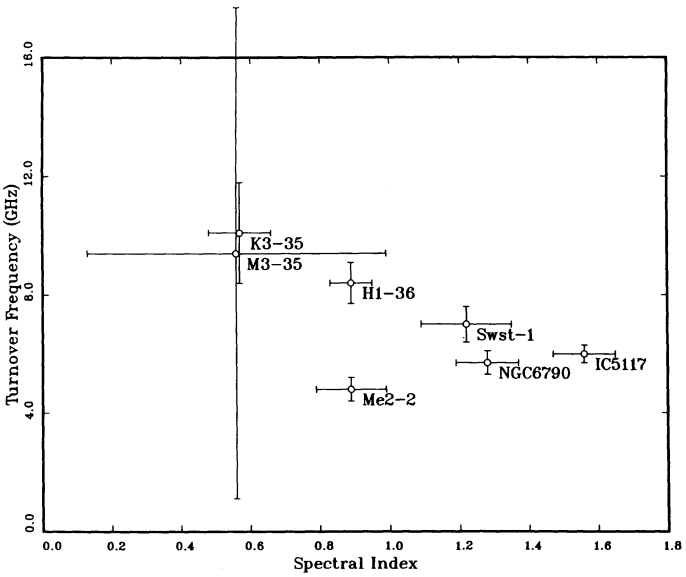

FIG. 4.—Critical frequency plotted against spectral index for seven of the compact nebulae.

with a ellipsoidal shell oriented at an angle to the observer. A number (~8 out of 18) of nebulae are observed to have low-surface-brightness halos outside of the shell component. This is probably due to the remnant of the AGB circumstellar envelope now being swept up by the newly formed planetary nebula shell. In the picture of the interacting stellar winds model of planetary nebulae formation, the relative brightness of the halo and shell components is expected to be higher in young systems. As a planetary nebula ages, the emission measure in the shell will increase at the expense of the halo. The halo can only be seen by optical CCD observations where the dynamic range is much higher than that in the radio. We also note that the halos appear more spherical than the shell, and this is again consistent with the interacting stellar winds model where the fast wind from the central star magnifies any density structure in the AGB wind (Balick 1987) making the shell structure more bipolar.

The spectral indices derived from the observed fluxes suggest that the spectral index of young planetary nebulae decreases as it evolves. The high critical frequencies and radio surface brightness of these objects suggest that they belong to a young population of planetary nebulae.

We thank C. R. Purton for communicating results of his radio measurements on some of these objects prior to publication. We also thank K. Volk and C. Y. Zhang for helpful discussions. This work is supported by a grant from the Natural Sciences and Engineering Research Council of Canada.

REFERENCES

Aaquist, O. B. 1991, in preparation
Aaquist, O. B., & Kwok, S. 1990, A&AS, 84, 229 (Paper I)
Acker, A., Gleizes, F., Chopinet, M., Marcout, J., Ochsenbein, F., & Roques, J. M. 1982, Publication speciale du CDS, No. 3
Acker, A., Marcout, J., & Ochsenbein, F. 1983, A&AS, 54, 315
Acker, A., Stenholm, B., & Tylenda, R. 1989, A&AS, 77, 487
Aitken, D. K., Roche, P. F., Spencer, P. M., & Jones, B. 1979, ApJ, 233, 925
Allen, D. A. 1983, MNRAS, 204, 113
Aller, L. H., & Czyzak, S. J. 1983, ApJS, 51, 211
Aller, L. H., & Keyes, C. D. 1987, ApJS, 65, 405
Balick, B. 1987, AJ, 94, 671
Barker, T. 1978, ApJ, 219, 914
Beckwith, S., Persson, S. E., & Gatley, I. 1978, ApJ, 219, L33
Bignell, R. C. 1983, IAU Symp. 103, Planetary Nebulae, ed. D. R. Flower (Dordrecht: Reidel), 69
Bryan, G. L., & Kwok, S. 1991, ApJ, 368, 252
Cerruti-Sola, M., & Perinotto, M. 1985, ApJ, 291, 237
de Freitas Pacheco, J. A., & Veliz, J. G. 1987, MNRAS, 227, 773
Dinerstein, H. L., Lester, D. F., Carr, J. S., & Harvey, P. M. 1988, ApJ, 327, L27
Eder, J., Lewis, B. M., & Terzian, Y. 1988, ApJS, 66, 183
Engels, D., Schmid-Burgk, J., Walmsley, C. M., & Winnberg, A. 1985, A&A, 148, 344
Feibelman, W. A., & Aller, L. H. 1987, ApJ, 319, 407
Flower, D. R., Goharji, A., & Cohen, M. 1984, MNRAS, 206, 293
French, H. B. 1983, ApJ, 273, 214
Gathier, R., Pottasch, S. R., & Goss, W. M. 1986, A&A, 157, 191
Greig, W. E. 1971, A&A, 10, 161
———. 1972, A&A, 18, 70
Gurzadyan, G. A. 1988, Ap&SS, 149, 343
Henize, K. G. 1967, ApJS, 14, 125
Higgs, L. A. 1971, Pub. Astr. Branch Nat. Res. Council of Canada, 1, 1
Huggins, P. J., & Healy, A. P. 1989, ApJ, 346, 201
Iijima, T. 1981, Photometric And Spectroscopic Binary Systems, Series C, Vol. 69, ed. E. B. Carling & Z. Kopal (Dordrecht: Reidel) 517
Isaacman, R. 1984, A&A, 130, 151
Johnson, H. M., Balick, B., & Thompson, A. R. 1979, ApJ, 233, 919
Kaler, J. B. 1976, ApJS, 31, 517
———. 1986, ApJ, 308, 322
Kohoutek, L., & Martin, W. 1981, A&A, 94, 365
Köppen, J. 1977, A&A, 56, 189
Kondrat'eva, L. N. 1978, Sov. Astr., 22, 194
Kwok, S. 1982, ApJ, 258, 280
Kwok, S. 1983, in IAU Symp. 103, Planetary Nebulae, ed. D. R. Flower (Dordrecht: Reidel), 293
———. 1985, AJ, 90, 49
Kwok, S., & Purton, C. R. 1979, ApJ, 229, 187
Kwok, S., Purton, C. R., & FitzGerald, P. M. 1978, ApJ, 219, L125
Kwok, S., Purton, C. R., & Keenan, D. W. 1981, ApJ, 250, 232
Leene, A., & Pottasch, S. R. 1988, A&A, 202, 203
Lewis, B. M., Eder, J., & Terzian, Y. 1987, AJ, 94, 1025
Masson, C. R. 1986, ApJ, 302, L27
Mendez, R. H., Kudritzki, R. P., & Simon, K. P. 1984, A&A, 142, 289
Milne, D. K. 1979, A&AS, 36, 227
Milne, D. K., & Aller, L. H. 1975, A&A, 38, 183
———. 1982, A&AS, 50, 209
Milne, D. K., & Webster, B. L. 1979, A&AS, 36, 169
Miranda, L. F., & Solf, J. 1989, A&A, 214, 353
Newell, R. T., Hjellming, R. M. 1981, BAAS, 13, 853
Panagia, N., & Walmsley, C. M. 1978, A&A, 411, 71
Payne, H. E., Phillips, J. A., & Terzian, Y. 1988, ApJ, 326, 368
Peimbert, M. 1978, IAU Symp. 76, Planetary Nebulae, ed. Y. Terzian (Dordrecht: Reidel), 215
Phillips, J. P. 1984, A&A, 140, 141
Pottasch, S. R. 1984, Planetary Nebulae (Dordrecht: Reidel)
Pottasch, S. R., et al. 1984, A&A, 138, 10
Purton, C. R., & Blackwell, S. R. 1991, in preparation
Purton, C. R., Feldman, P. A., Marsh, K. A., Allen, D. A., & Wright, A. E. 1982, MNRAS, 198, 321
Sabbadin, F. 1986, A&AS, 65, 301
Sanduleak, N. 1975, Pub. Warner and Swasey Obs., Vol. 2, No. 1
Schneider, S. E., Silverglat, P. R., Altschuler, D. R., & Givanardi, C. 1987, ApJ, 314, 572
Schneider, S. E., Terzian, T., Purgathofer, A., & Perinotto, M. 1983, ApJS, 52, 399
Stenholm, B., & Acker, A. 1987, A&AS, 68, 51
Taylor, A. R. 1988, in the Symbiotic Phenomenon, ed. J. Mikolajewska, M. Friedjung, S. Kenyon, & R. Viotti (Dordrecht: Kluwer), 77
Taylor, A. R., Gussie, G. T., & Pottasch, S. R. 1990, ApJ, 351, 515
Turner, C., & Terzian, Y. 1984, AJ, 89, 501
Tylenda, R., Acker, A., Gleizes, F., & Stenhom, B. 1989, A&AS, 77, 39
Wright, A. E., & Barlow, M. J. 1975, MNRAS, 170, 41
Zhang, C. Y., & Kwok, S. 1990, A&A, 237, 479
———. 1991, A&A, in press
Zuckerman, B., & Aller, L. H. 1986, ApJ, 301, 772